Electronic Supplementary Material (ESI) for Journal of Materials Chemistry A.

Electronic Supplementary Information

Tailored near-infrared-emitting colloidal heterostructured quantum dots with enhanced visible light absorption for high performance photoelectrochemical cells

Ali Imran Channa[a], Xin Tong[a*], Jing-Yin Xu[a], Yongchen Liu[a], Changmeng Wang[a], Muhammad Naeem Sial[a], Peng Yu[a], Haining Ji[b], Xiaobin Niu[b], Zhiming M. Wang[a*]

a. Institute of Fundamental and Frontier Sciences, University of Electronic Science and Technology of China, Chengdu 610054, P. R. China

b. School of Materials and Energy, State Key Laboratory of Electronic Thin Film and Integrated Devices, University of Electronic Science and Technology of China

Corresponding authors: xin.tong@uestc.edu.cn; zhmwang@uestc.edu.cn

Experimental Section

Materials

Copper(I) Iodide (CuI) (≥99.99%), Gallium(III) Iodide (GaI_3) (≥99.99%), Sulfur (S)(≥99.99%),Cadmium Oxide (CdO), Oleylamine (OLA) (Technical grade, 70%), 1-Octadecene (ODE) (Technical grade, 90%), 1-Dodecanethiol (DDT), Trioctylphosphine (TOP) (97%), Sodium Sulfide (Na_2S), Sodium Sulfite (Na_2SO_3), Hexadecyltrimethylammonium bromide (CTAB), Toluene, Methanol, Acetone were purchased from Sigma-Aldrich Inc. Titania 18NR-AO paste consisting of a mixture of active anatase particles of size ~20 nm diameter and larger anatase scattering particles up to ~450 nm in diameter was obtained from Dyesol (Queanbeyan, Australia) Ti-Nanoxide BL/SC was purchased from Solaronix. All the chemicals were utilized as purchased.

Synthesis of CGS core QDs

CGS core QDs were synthesized by using a wet colloidal technique reported in literature with slight modifications[1]. The synthetic processes were carried out in a Schlenk line system under N_2 purging as illustrated in **Figure S1**. In a typical synthesis, 0.25 mmol of CuI, 0.25 mmol of GaI_3 and 2.5 mL of OLA were placed in a three-neck flask with a magnetic stirrer. The reaction mixture was then heated to 60 ^{o}C with N_2 purging and vacuum pumping until the color turns to dark green. 0.25 mL of DDT was then injected into the solution and the solution subsequently turned to a clear light yellow color and then quickly turned opaque milky. At this stage the temperature was increased to 125 ^{o}C. When the temperature reached above 115 ^{o}C, the color of the solution started to turn light yellow but opaque. The solution turned to a transparent light yellow colour at 125 ^{o}C. The solution was degassed at this stage in N_2 environment for about 30 min.

In the meantime, sulfur stock solution was prepared by loading 1 mmol of sulfur with 1.5 mL of ODE in a separate three-neck flask with a magnetic stirrer. This mixture was first degassed at 120 ^{o}C for 30 min and heated at 200 ^{o}C for 30 min. This sulfur solution was injected into the above reaction mixture at 180 ^{o}C and maintained at this temperature for 5 min for the nucleation of core QDs. The temperature was then increased to 220 ^{o}C for 30 min and the reaction was stopped by quenching with water bath. For the purification of core QDs, the original QDs were first diluted with toluene and centrifuged at ~3000 r.p.m to get rid of the unreacted precursor and bulk materials. The residue was thrown and the supernatant (QDs solution) was then washed with ethanol and re-dispersed in toluene.

Synthesis of CGS/CdS core/shell QDs

For the growth of CGS/CdS core/shell QDs, a CdS stock solution was first prepared. For this 1 mmol of sulfur was dissolved in 1 mL of TOP and 4 mL ODE. 1.5 mL of this solution was then mixed with 1.5 mL of Cd-oleate. 2 mL of original core QDs were purified using the method described above. After purification, the QDs were diluted by 5 mL of ODE and loaded into a three-neck flask with a magnetic stirrer. This mixture was then degassed and purged by N_2 first at 60 ^{o}C and then at 120 ^{o}C for 30 min. The temperature was subsequently increased to 180 ^{o}C and 3 ml of CdS stock solution was injected slowly using a syringe pump with an injection rate of 0.066 mL/min. After initiating the injection, the temperature was increased to 215 ^{o}C and maintained at this temperature. After the injection was completed, the reaction was quenched by water bath. The core/shell QDs were also purified using the same method described above and stored in toluene at -5 ^{o}C for further characterizations.

PEC device preparation

Preparation of TiO_2 film: In order to prepare the TiO_2 film, FTO coated glass substrates were washed sequentially by acetone, ethanol and de-ionized water for 30 min in an ultrasonic machine and dried using N_2 gas. A compact TiO_2 layer was spin-coated on FTO glass substrates at 5000 r.p.m for 30 s using Ti-Nanoxide BL/SC. The substrates were then annealed in air at 500 ^{o}C for 30 min. Afterwards, Titania paste 18NR-AO was deposited on the TiO_2 compact layer by tape casting. The substrates were first dried in air for 13 min followed by heating on hot plate at 120 ^{o}C for 6 min. The substrates were then sintered in a furnace at 500 ^{o}C with ramp rate of 5 ^{o}C/min for 30 min in air.

Sensitization of QDs in mesoporous-TiO_2 film: The QDs were sensitized in mesoporous-TiO_2 film by the process of electrophoretic deposition (EPD). In this process, two substrates with the TiO_2 films facing each other were immersed vertically in QDs solution. The distance between the substrates was kept to be 1 cm. A direct current (DC) bias source of 100 V was applied on these photoanodes for 60 min. The photoanodes were then washed by toluene several times to remove unbound QDs and dried by N_2 gas. For ligand exchange, the photoanodes were then kept in CTAB solution (0.2 g in 20 mL methanol) for 1 min subsequently washed by methanol and dried by N_2. This process was repeated twice.

ZnS protection layer: In order to protect the photoanodes from photocorrosion, the surface treatment was performed by the deposition of ZnS capping layer using successive ionic layer adsorption and reaction (SILAR) method. In a typical ZnS SILAR deposition process, 0.1 M solution of $Zn(Ac)_2$ (in methanol) acts as a source of Zn^{2+} and 0.1 M solution of Na_2S (in methanol:DI-water 1:1) acts as a source of S^{2-}. One SILAR cycle involves the sequential dip-coating of photoanodes for 1 min in Zn^{2+} solution and 1 min in S^{2-} solution. After each dip-coating, the photoanodes were rinsed thoroughly by the corresponding solvents (methanol or methanol: DI-water) to get rid of the residual chemicals and dried by N_2. For all photoanodes, two cycles of SILAR were employed.

Characterization

Transmission electron microscopy (TEM), selected area electron diffraction (SAED) and energy dispersive x-rays (EDS) mapping of QDs were acquired using a JEM 2100F TEM. The X-ray diffraction (XRD) pattern was obtained by utilizing a D8 ADVANCE X-ray Diffractometer from Bruker with Cu-Kα radiation. UV–visible–NIR absorption spectra were measured by using UV-Vis spectrophotometer (Shimadzu UV-3101 PC). Photoluminescence (PL) spectra and PL lifetime of the QDs in solution were acquired via a FLS 920 fluorescence spectrometer equipped with an InGaAs NIR detector (Edinburgh Instrument, UK). The morphology of the cross-section FTO/TiO_2/QDs was attained by using a FEI Inspect F50 scanning electron microscope (SEM) and the chemical composition mapping was obtained by EDS analysis. X-ray photoelectron spectroscopy (XPS) scan was obtained by ULVAC-PHI, PHI Quantro SXM system. A three-electrode system consisting of an Ag/AgCl reference electrode (saturated with KCl), a Pt counter electrode, and an as-fabricated working electrode was used to evaluate the photoelectrochemical (PEC) performance of the QD-sensitized photoanode. The photoanode was dipped into the electrolyte consisting of 0.25 M Na_2S and 0.35 M Na_2SO_3 (pH = ~13), serving as sacrificial hole scavenger to prevent QDs from photo-corrosion. Photocurrent density–voltage (J–V) measurements were conducted under simulated one sun illumination (1 Sun = AM 1.5G, 100 mW cm^{-2}) using a Class AAA Solar Simulator (SAN-EI, XES-50S1) and an electrochemical workstation (PARSTAT 3000A-DX with 20 mV/s sweep rate). A Si reference diode was used to calibrate the distance between photoelectrode and solar simulator before each measurement and the distance from sun simulator to PEC cell was kept ~12 cm. In order to convert the measured potentials V (V vs AgCl) into V_{RHE} (V versus reversible hydrogen electrode) the equation $V_{RHE} = V_{Ag/AgCl} + 0.197 + pH \times 0.059$ was used. The evolution of hydrogen gas was measured using a gas chromatographer (GC) (Shimadzu GC-2014) and the samples for measurement were collected using an airtight syringe.

Synthesis Scheme

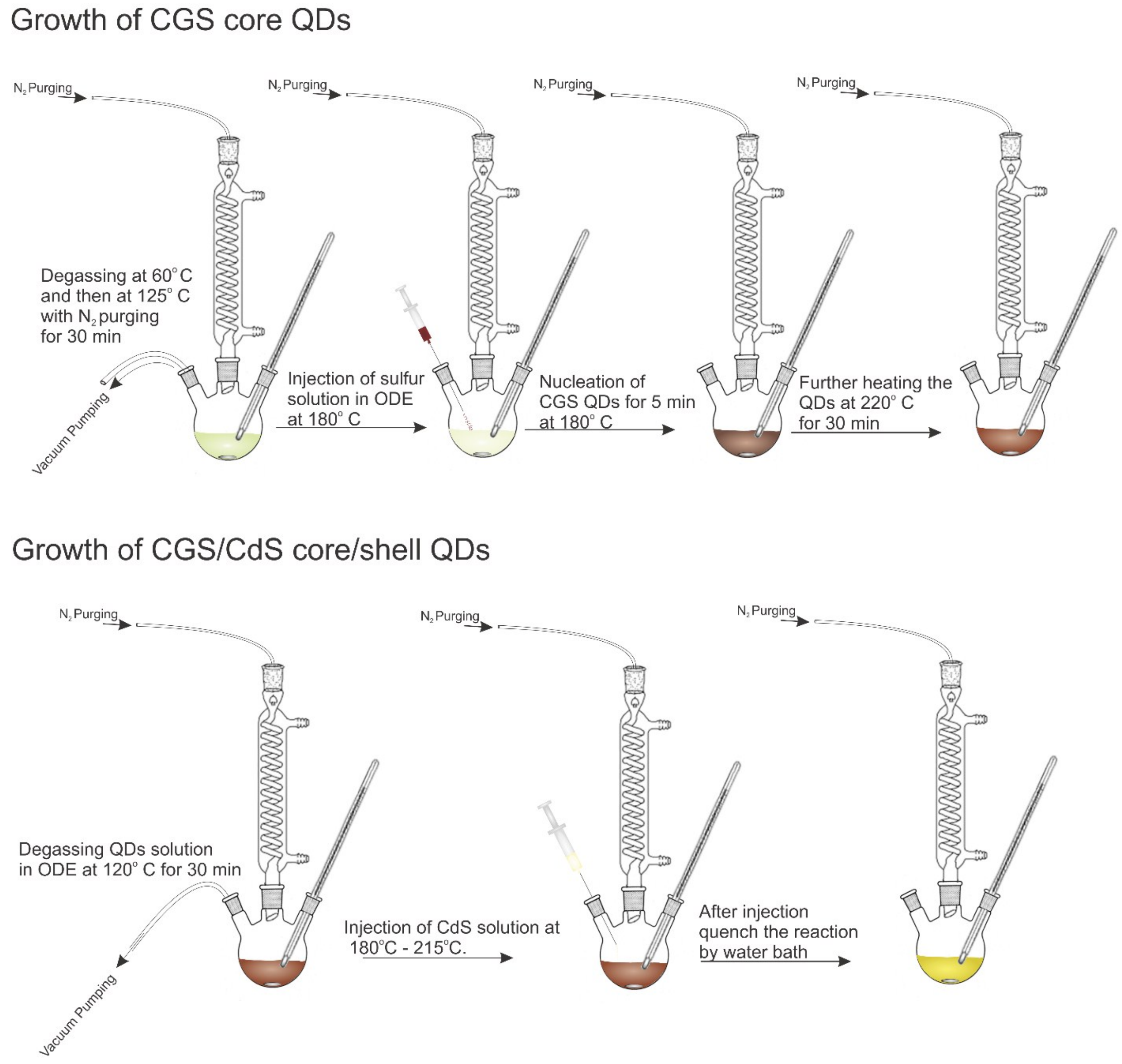

Figure S1. Synthetic schemes of CGS core and CGS/CdS core/shell QDs.

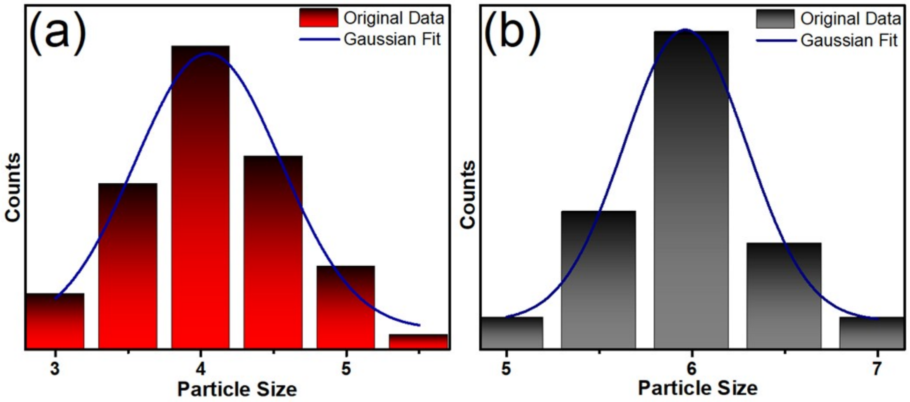

Figure S2. Size distribution of (a) CGS core and (b) CGS/CdS core/shell QDs, showing average sizes of 4 ± 0.6 nm and 6 ± 0.4 nm, respectively.

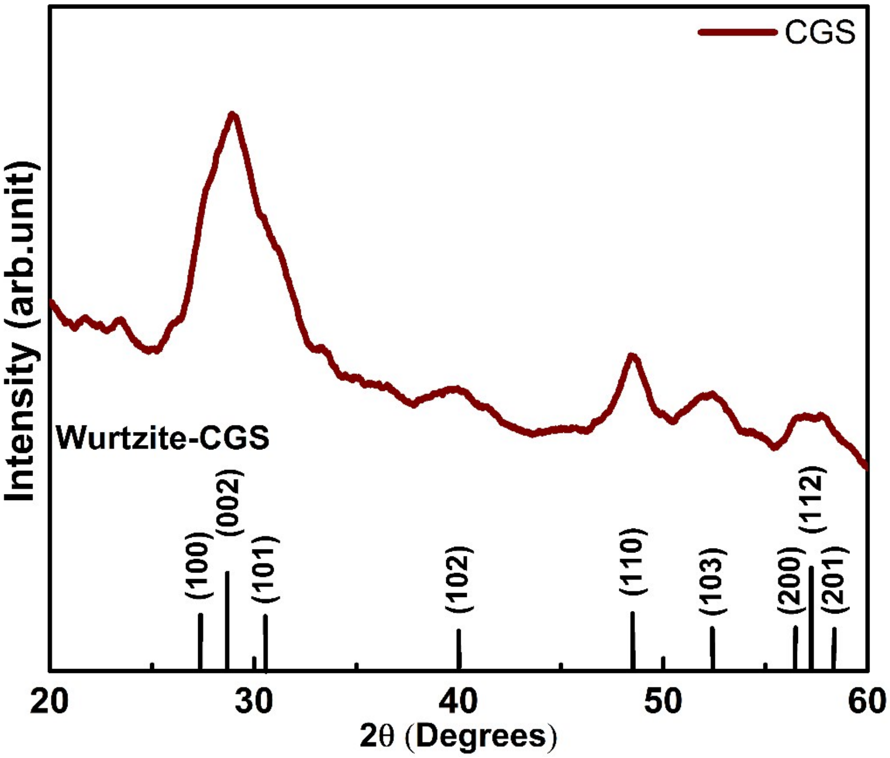

Figure S3. X-ray diffraction spectrum of bare CGS core QDs exhibiting wurtzite phase.

Lattice parameter calculation

In order to calculate the lattice parameters following two equations were used

$$2d\sin\theta = n\lambda \text{ ------------------------ (Equation S1)}$$

$$\frac{1}{d^2} = \frac{4}{3}\left(\frac{h^2 + hk + k^2}{a^2}\right) + \frac{l^2}{c^2}$$ **---------- (Equation S2)**

Where in equation S1, *d* is the interplanar distance, θ is the Bragg's angle, n is positive integer and λ is the x-ray wavelength. In equation S2, *d* is the interplanar distance, h,k,l are miller indices, *a* and *c* are lattice parameters for wurtzite crystal structure.

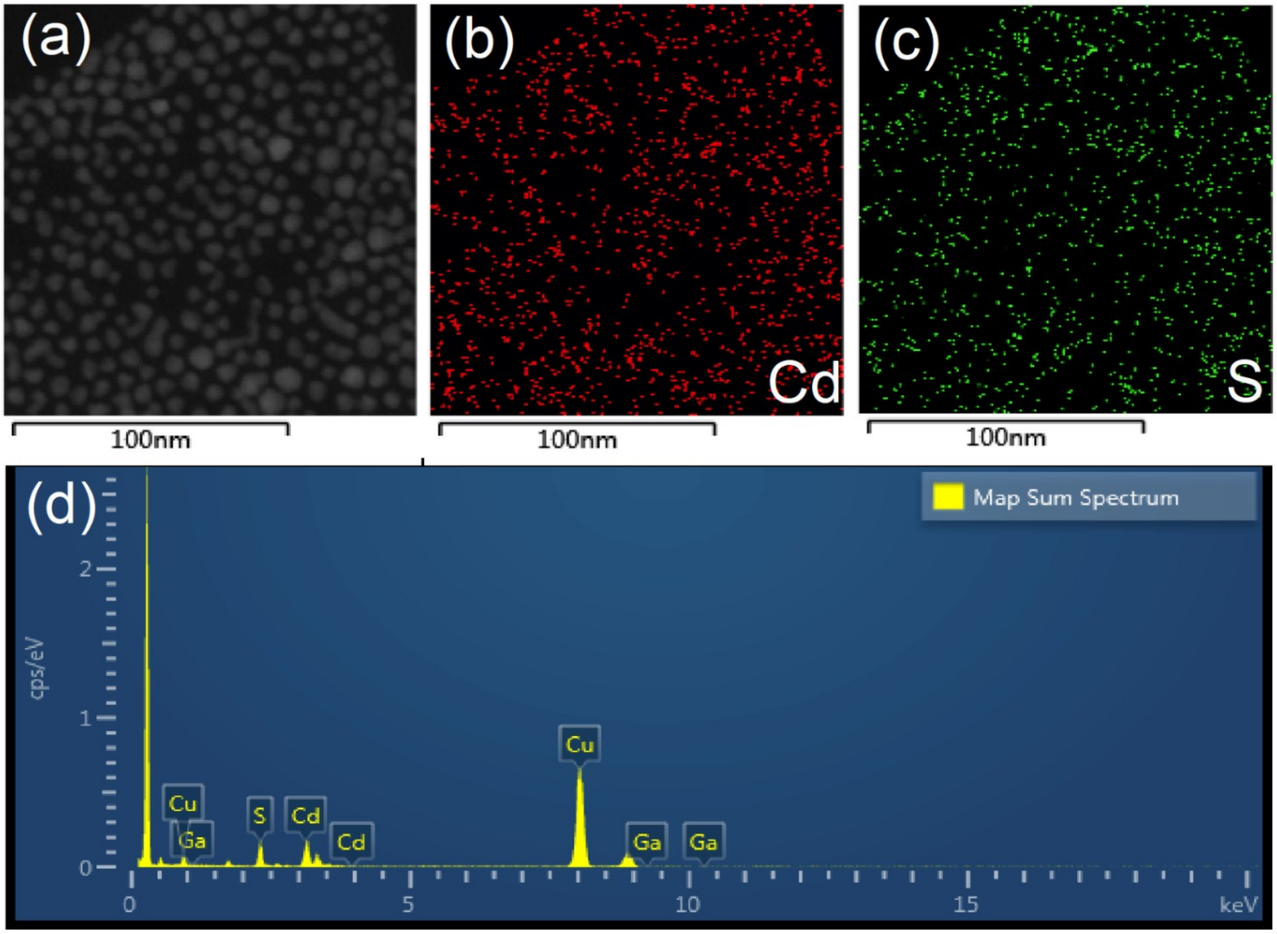

Figure S4. EDS mapping and spectrum obtained for CGS core/shell QDs showing the corresponding detected elements.

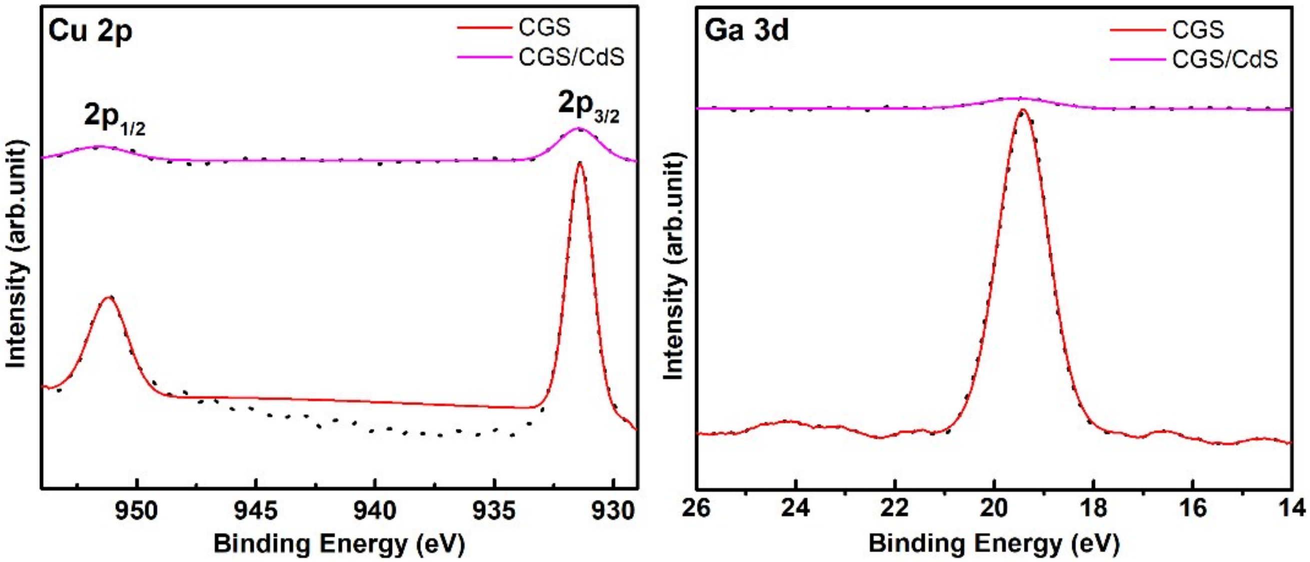

Figure S5. High resolution x-ray photoelectron spectroscopy (XPS) spectrum obtained from CGS core QDs and CGS/CdS core/shell QDs. Both core and core/shell QDs XPS spectra have same peak positions with core/shell QDs exhibiting attenuated XPS signal intensity after the formation of CdS shell.

Tauc equation:

$$\alpha hv \propto (hv - E_g)^n$$ **------------------ (Equation S3)**

where α is the absorption coefficient or absorbance, h is the Planck constant, v is the frequency, $hv = 1240/\lambda$, and E_g is the optical band gap of QDs. Exponent n is a constant and denotes the nature of the transition in the band gap and can have values of

n = ½ direct allowed

n = 2 indirect allowed

n = 3 indirect forbidden

n = 3/2 direct forbidden transition

In our case, we selected the value of 1/2 for direct allowed transition.

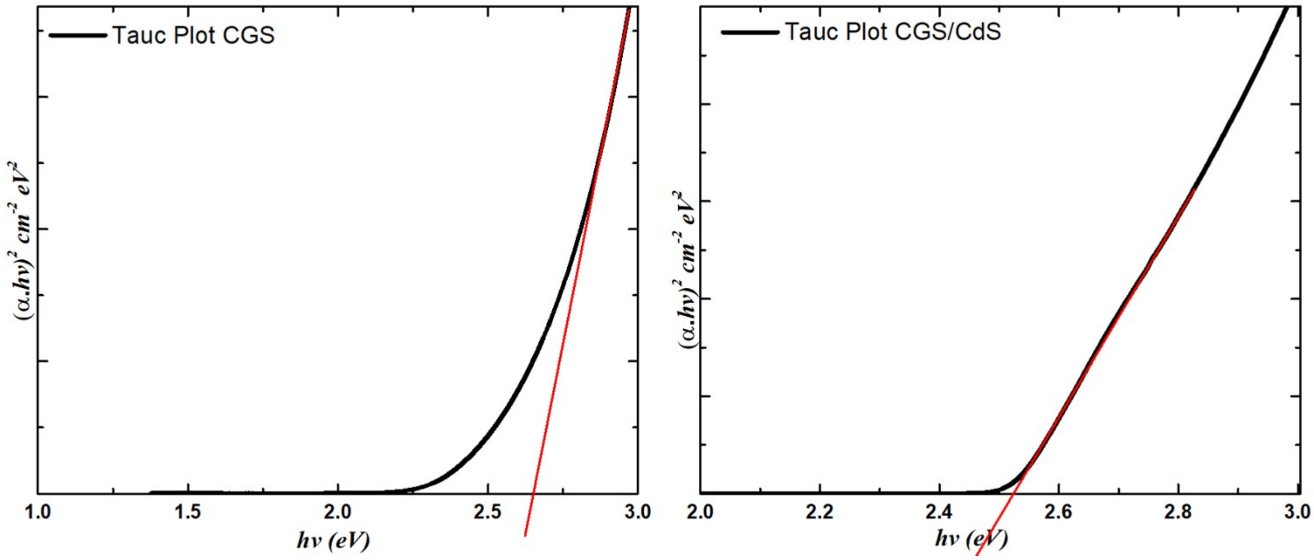

Figure S6. Tauc plots for CGS core and CGS/CdS core/shell QDs.

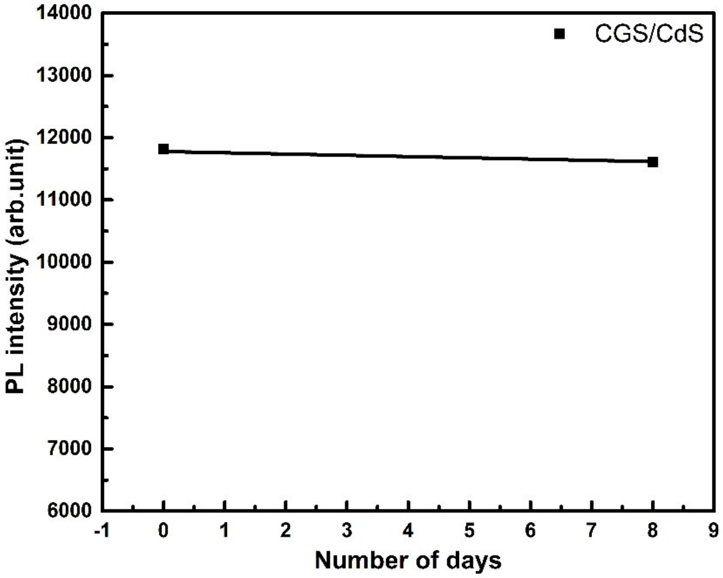

Figure S7. PL intensity as a function of time for CGS/CdS core/shell QDs. In order to observe the photo-stability of the CGS/CdS core/shell QDs, the PL spectrum was recorded from the same sample with a difference of 8 days. It was observed that the sample retained its PL intensity even after 8 days.

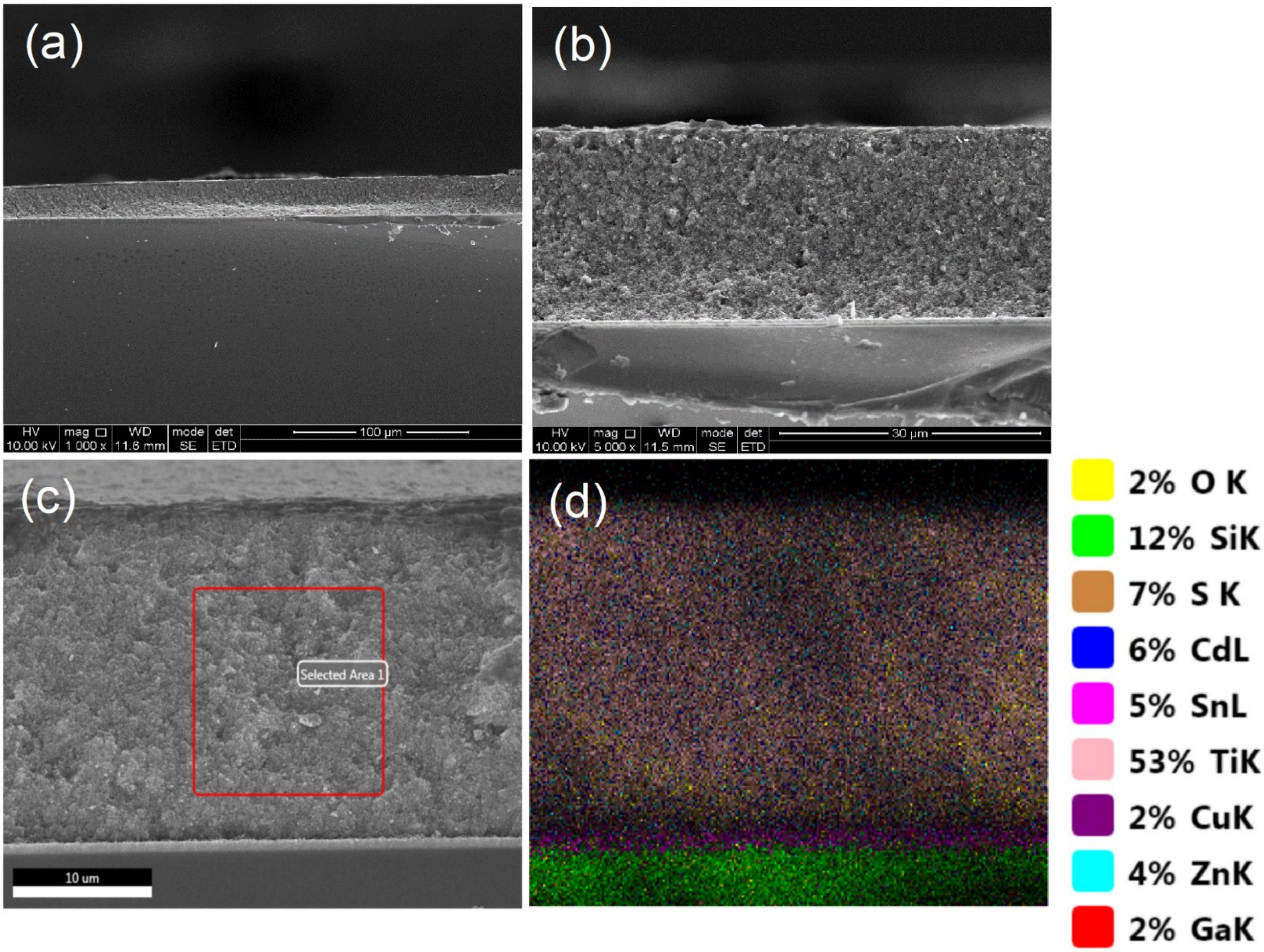

Figure S8. (a-b) Cross-sectional SEM images of photoanode with different resolutions. (c) Red box indicates the region where the EDS mapping was conducted. (d) Colored mapping of device cross section, showing the uniform distribution of QDs in mesoporous-TiO_2 film.

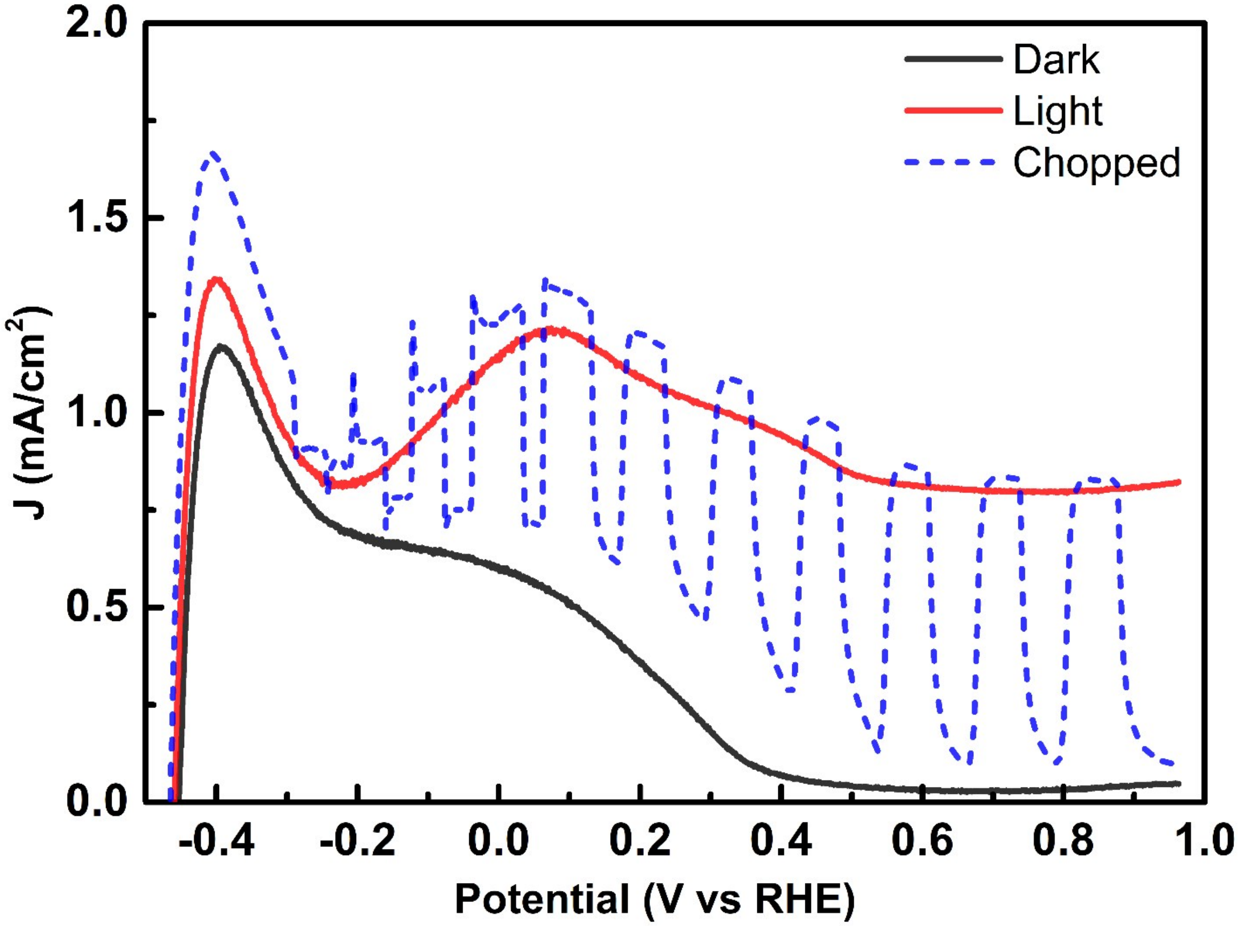

Figure S9. Linear sweep voltammetry of CGS core QDs-based photoanode in dark, continuous and chopped light under 1 sun illumination (AM 1.5G, 100 mW/cm^2) displaying the current density of about ~0.83 mA/cm^2.

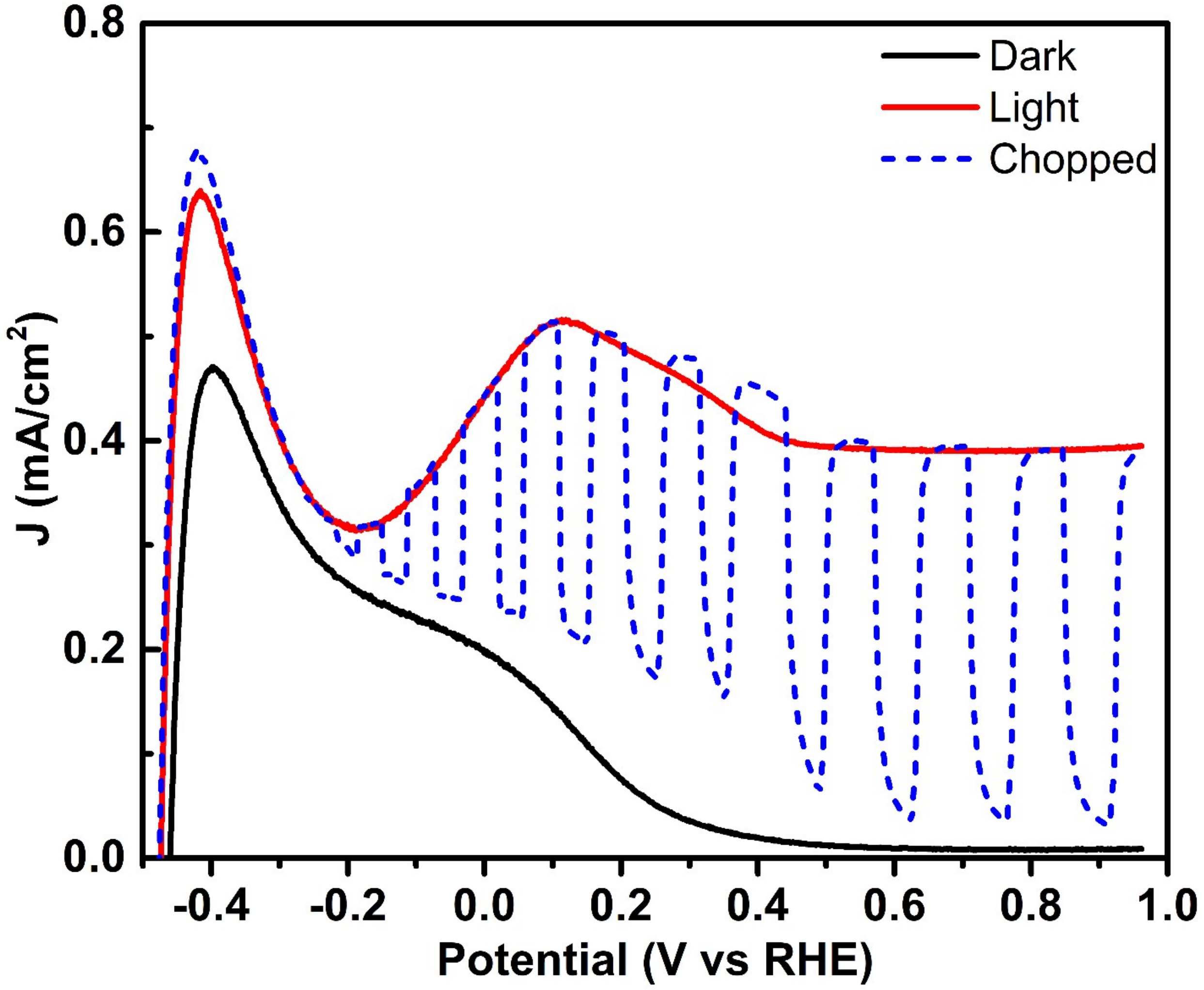

Figure S10. Linear sweep voltammetry of bare mesoporous-TiO_2 -based photoanode in dark, continuous and chopped light under 1 sun illumination (AM 1.5G, 100 mW/cm^2) displaying the current density of about ~0.39 mA/cm^2.

Table S1. Comparison of CGS/CdS core/shell QDs based PEC cell with other QDs based PEC cells.

Type of QDs	**Photocurrent Density (mA/cm^2)**	**Stability of Device**	**Faradaic Efficiency (FE)**	**Reference**
CGS/CdS	~6.5	~ 60%	~50%	Current work
Zn-CuInSeS	~4.27	~ 77%	-	[2]
CuInSeS/CdSeS/CdS#6	~5.5	~60%	-	[3]
CdSe/CdS giant-QDs	~10	~52%	-	[4]
PbS/CdS giant-QDs	~ 5.3	~78%	-	[5]
CdSe/CdS	~4.7	~96%	-	[6]

The following reactions explain the possible phenomena at the interface of electrode-electrolyte[7-10].

$$CGS/CdS/TiO_2 + h\upsilon \longrightarrow h^+ + e^-$$

$$2e^- + 2H_2O \longrightarrow H_2 + 2OH^-$$

$$2SO_3^{2-} + 2OH^- + 2h^+ \longrightarrow 2SO_4^{2-} + 2H^+$$

$$2S^{2-} + 2h^+ \longrightarrow S_2^{2-}$$

$$S_2^{2-} + SO_3^{2-} \longrightarrow S_2O_3^{2-} + S^{2-}$$

$$SO_3^{2-} + S^{2-} + 2h^+ \longrightarrow S_2O_3^{2-}$$

The amount of hydrogen was estimated and the result is shown in Figure S11 below. The theoretical value of hydrogen was calculated from the I×t curve by following formula[11]

$$H_2\,(\text{mole}) = \frac{Q}{2F} = \frac{I \times t}{2F} = \frac{1}{2}\int_0^t \frac{Idt}{F}$$

Here, *I* is the photocurrent of the photoanode, Q is the quantity of charge passed in time t and F is the Faradays constant (96484.34 C/mol). Q can be calculated by *I* × t, but in case if the current is not constant, then the amount of charge can be estimated by integrating the current (*I*) over time (t). Based on these results the Faraday efficiency was calculated by using following formula and was found to be around ~50%.

$$F.E = \frac{Experimental\ value\ of\ H_2}{Theoretical\ Value\ of\ H_2}$$

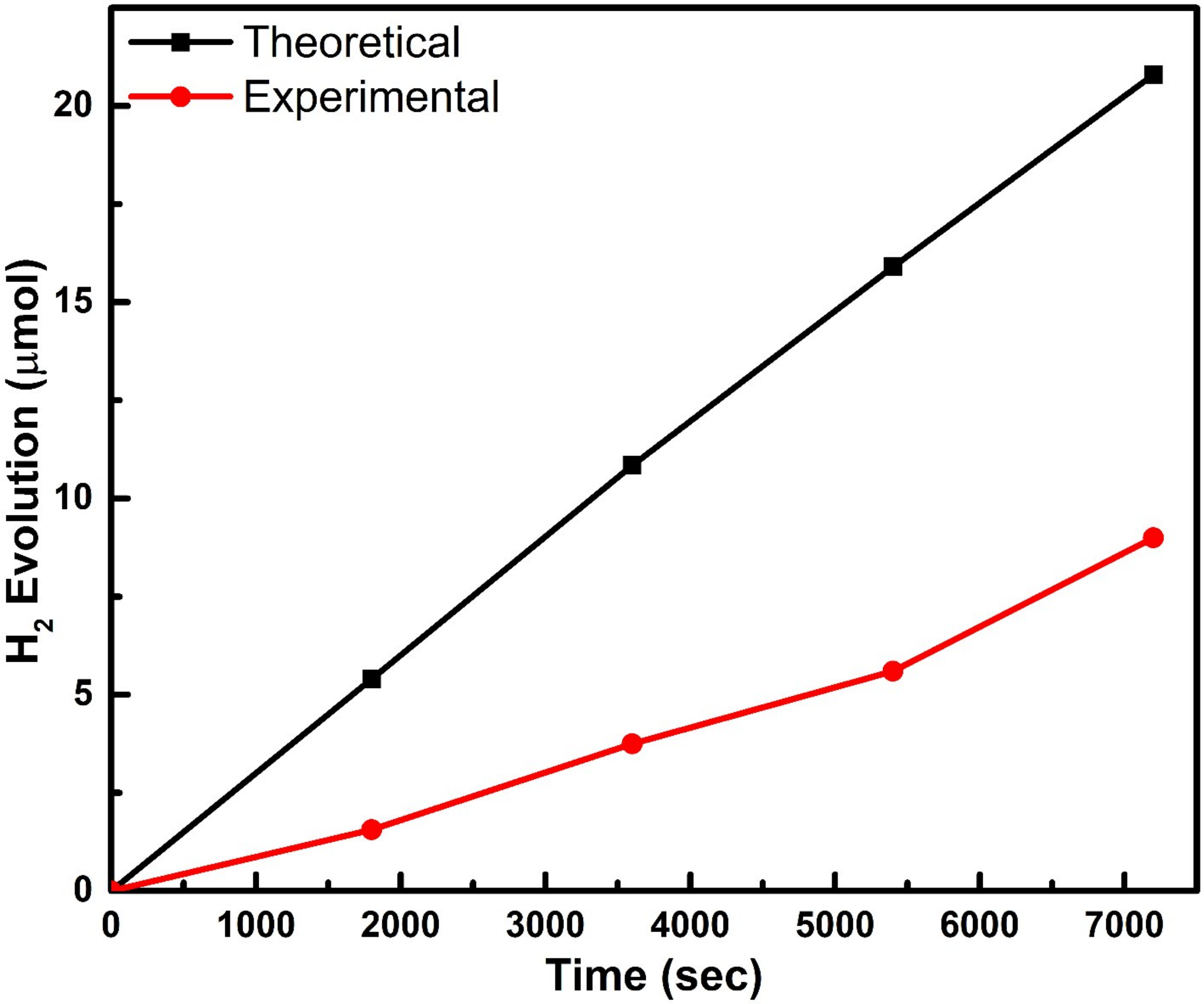

Figure S11.Hydrogen generation from the CGS/CdS core/shell QDs based photoanode. Theoretical amount of hydrogen was calculated using the measured photocurrent, whereas, experimental value was determined by employing GC system.

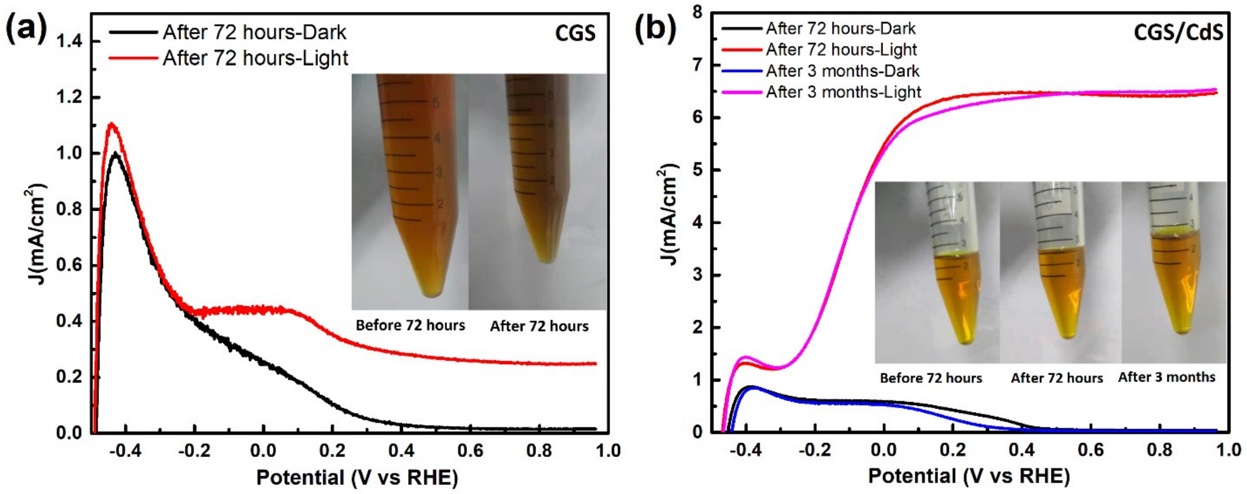

Figure S12.PEC performance of (a) CGS core QDs and (b) CGS/CdS core/shell QDs measured at different time intervals.

References

1. M. Jalalah, M. S. Al-Assiri and J.-G. Park, *Adv. Energy Mater.*, 2018, **8**, 1703418.
2. X. Tong, Y. Zhou, L. Jin, K. Basu, R. Adhikari, G. S. Selopal, X. Tong, H. Zhao, S. Sun, A. Vomiero, Z. M. Wang and F. Rosei, *Nano Energy*, 2017, **31**, 441-449.
3. X. Tong, X.-T. Kong, C. Wang, Y. Zhou, F. Navarro-Pardo, D. Barba, D. Ma, S. Sun, A. O. Govorov, H. Zhao, Z. M. Wang and F. Rosei, *Adv. Sci.*, 2018, **5**, 1800656.
4. R. Adhikari, L. Jin, F. Navarro-Pardo, D. Benetti, B. AlOtaibi, S. Vanka, H. Zhao, Z. Mi, A. Vomiero and F. Rosei, *Nano Energy*, 2016, **27**, 265-274.
5. L. Jin, G. Sirigu, X. Tong, A. Camellini, A. Parisini, G. Nicotra, C. Spinella, H. Zhao, S. Sun, V. Morandi, M. Zavelani-Rossi, F. Rosei and A. Vomiero, *Nano Energy*, 2016, **30**, 531-541.
6. K. Basu, H. Zhang, H. Zhao, S. Bhattacharya, F. Navarro-Pardo, P. K. Datta, L. Jin, S. Sun, F. Vetrone and F. Rosei, *Nanoscale*, 2018, **10**, 15273-15284.
7. N. Bao, L. Shen, T. Takata and K. Domen, *Chem. Mater.*, 2008, **20**, 110-117.
8. X. Chen, S. Shen, L. Guo and S. S. Mao, *Chem. Rev.*, 2010, **110**, 6503-6570.
9. A. Kudo, I. Tsuji and H. Kato, *Chem. Commun.* , 2002, DOI: 10.1039/B204259B, 1958-1959.
10. I. Tsuji, H. Kato, H. Kobayashi and A. Kudo, *J. Am. Chem. Soc.*, 2004, **126**, 13406-13413.
11. B. AlOtaibi, H. P. T. Nguyen, S. Zhao, M. G. Kibria, S. Fan and Z. Mi, *Nano Lett.*, 2013, **13**, 4356-4361.